Table 1 Convergence study for Beck's column, $L/r = 10$

Number of elements	Q_{cr} Linear γ	Cubic γ
1	5.954	3.876
2	1.301	1.047
4	1.063	1.032
8	1.035	1.023
16	1.024	. . .

Table 2 Critical loads for Beck's column, 8-element solution (cubic γ)

L/r	Q_{cr}	λ^2_{cr}
10	1.023	46.1
15	1.400	71.7
25	1.742	97.6
50	1.949	114
100	2.010	119
1000	2.032	121

Table 3 Convergence study for Leipholz' problem: cubic γ; $L/r = 10$

Number of elements	Q_{cr}
1	8.167
2	2.140
4	1.839
8	1.813

Table 4 Critical loads for Leipholz's problem: 8-element solution (cubic γ)

L/r	Q_{cr}	λ^2_{cr}
10	1.813	44.5
15	2.636	70.9
25	3.406	97.6
50	3.871	114
100	4.012	119
1000	4.059	121

and

$$W^{Nc} = -P(w_x + \gamma)|_{x=l}\, w(l) \quad \text{for Beck's column} \tag{6}$$

$$= -p\int_0^l (w_x + \gamma)\, w dx \quad \text{for Leipholz's column} \tag{7}$$

In the above expression ψ_x is the curvature, A is the area of cross section, r is the radius of gyration, w is the lateral displacement, γ is the shear rotation, and ν is the Poisson's ratio. Suffix x denotes differentiation with respect to the axial coordinate x.

For the derivation of the element matrices, w is assumed as cubic in x with nodal parameters w and w_x at each note. For γ two distributions are used: 1) a linear distribution with γ as a nodal parameter, and 2) a cubic distribution with γ and γ_x as nodal parameters.

Critical loads Q_{cr} are obtained with use of the dynamic criterion where the first two frequencies coalesce.

Numerical Results

Critical loads for Beck's column and Leipholz's column are obtained for various L/r ratios.

Table 1 shows the convergence study for 1- to 16-element solutions with both linear and cubic γ distribution for $L/r = 10$. From this table it is evident that the cubic displacement distribution for γ gives very accurate results even with 4 elements. Table 2 gives the critical loads and frequencies of coalescence λ^2_{cr} corresponding to a model with 8 elements and cubic γ. The results for $L/r = 1000$ agrees with the value given in Ref. 5.

Table 3 gives the convergence study for the Leipholz's column with cubic γ. The 8-element model gives satisfactory results. Table 4 gives the critical loads and coalescence frequencies for Leipholz's column with 8 elements and cubic γ. Again, the results obtained in the present study for $L/r = 1000$ agree very well with those of Ref. 5.

Concluding Remarks

From the results obtained in the present study the following conclusions can be drawn: 1) a cubic γ distribution gives very accurate results compared to a linear γ distribution; 2) for small L/r the reduction in critical load is significant; and 3) except for very small L/r the coalescence frequencies for a given L/r are the same for both Beck's column and Leipholz's column.

References

[1] Bolotin, V.V., *Nonconservative Problems of the Theory of Elasticity*, Pergamon Press, Oxford, 1963.

[2] Leipholz, H., *Stability Theory*, Academic Press, New York, 1970.

[3] Barsoum, R.S., "Finite Element Method Applied to the Problem of Stability of a Nonconservative System," *International Journal of Numerical Methods in Engineering*, Vol. 3, 1971, pp. 63-87.

[4] Kikuchi, F., "A Finite Element Method for Non-Self-Adjoint Problems," *International Journal of Numerical Methods in Engineering*, Vol. 6, 1973, pp. 39-54.

[5] Venkateswara Rao, G. and Narasimha Rao, R.V., "Galerkin Finite Element Solution for the Stability of Cantilever Columns Subjected to Follower Forces," *AIAA Journal*, Vol. 13, May 1975, pp. 690-691.

[6] Venkateswara Rao, G., Raju, I.S., and Kanaka Raju, K., "Nonlinear Vibrations of Beams Considering Shear Deformation and Rotatory Inertia," *AIAA Journal*, Vol. 14, May 1976, pp. 685-687.

[7] Zienkiewicz, O.C., *Finite Element Method in Engineering Science*, McGraw-Hill, New York, 1971.

J80-026

Stress Analysis of a Plate Containing Two Circular Holes Having Tangential Stresses

80004
80008

Vijay G. Ukadgaonker*
Indian Institute of Technology, Bombay, India

Introduction

IN this Note an elastostatic problem is solved using the procedure of Kolosoff-Muskhelishvili complex stress functions[1] and the Schwarz alternating method[2] of successive relaxation for multiplying connected regions. Using this technique the problem of stresses in an infinite plate with two rigid circular inclusions are solved by the author.[3,4]

This method is used for finding the stress field induced in an isotropic homogeneous infinite plate with two circular

Received Feb. 8, 1978; revision received June 7, 1979. Copyright © American Institute of Aeronautics and Astronautics, Inc., 1979. All rights reserved.

Index categories: Structural Statics; Structural Design.

*Lecturer, Mechanical Engineering Department.

holes (of radii a and b, which are c distance apart) having uniform tangential stresses of respective magnitudes T_1 and T_2 acting around them in a anticlockwise direction, as shown in Fig. 1. These tangential stresses will give the stress resultant on the respective boundaries as

$$f(t_1) = -i\int_{C_1} (T_1 \sin\theta_1 - iT_1 \cos\theta_1)\,ds$$

$$= iT_1 t_1 \qquad \text{on hole } C_1 \tag{1}$$

and

$$f(t_2) = iT_2 t_2 \qquad \text{on hole } C_2 \tag{2}$$

First Approximation

A first approximation to the stress field will be the superposition of two single hole solutions. The stress functions valid near the hole of radius a are obtained by solving Cauchy integrals as

$$\phi_1(z_1) = 0 \text{ and } \psi_1(z_1) = -iT_1 d^2/z_1 \tag{3}$$

where the z_1 plane corresponds to the center of hole C_1 of radius a. Similarly the stress functions valid near the hole of radius b are

$$\phi_2(z_2) = 0 \text{ and } \psi_2(z_2) = -iT_2 b^2/z_2 \tag{4}$$

where the z_2 plane corresponds to the center of hole C_2 of radius b.

Second Approximation

Starting from hole C_1, to account for the interaction effect of the two holes the stress functions (3) are transformed to $z_1 = c$ by the transformation $z_1 = z_2 + c$. The condition of invariance of stresses gives the transformed stress functions as

$$\phi_{12}(z_2) = \phi_1(z_1) = 0$$

$$\psi_{12}(z_2) = \psi_1(z_1) + c\phi'_{12}(z_2) = -iT_1 a^2/(z_2 + c) \tag{5}$$

These will lead to a boundary value f_{12} on C_2 which is not the required boundary condition. Hence the corrected stress resultant f_2 on C_2 is obtained in the form

$$f_2(t_2) = iT_2 t_2 - f_{12}(t_2) = iT_2 t_2 - iT_1 a^2 t_2/(b^2 + ct_2) \tag{6}$$

which gives the corrected complex stress functions on C_2 as

$$\phi_{22}(z_2) = \frac{iT_1 a^2 b^2}{c(cz_2 + b^2)}$$

and

$$\psi_{22}(z_2) = -\frac{iT_2 b^2}{z_2} + \frac{iT_1 a^2}{c} + \frac{iT_1 a^2 b^2}{z_2(cz_2 + b^2)^2} \tag{7}$$

Thus the stress functions which are valid in the neighborhood of hole of radius b are expressed as the sum of the transformed stress functions (5) and the corrected ones in Eq. (7):

$$\phi_2(z_2) = \phi_{12}(z_2) + \phi_{22}(z_2) = \frac{iT_1 a^2 b^2}{c(cz_2 + b^2)}$$

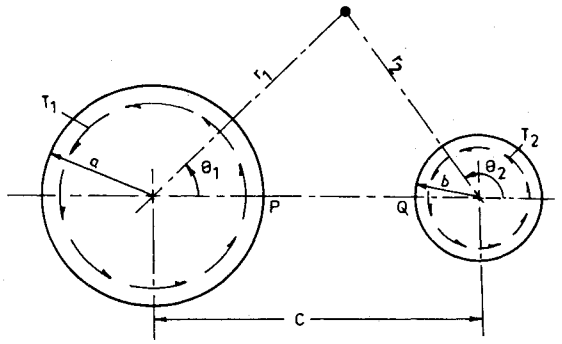

Fig. 1 Infinite plate with two holes.

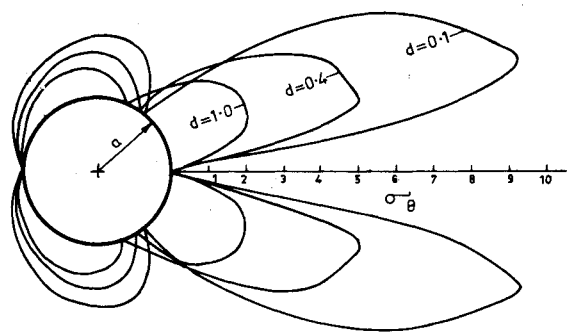

Fig. 2 σ_θ around a hole of radius a where $a = b$, $T_1 = T_2 = 1.0$.

and

$$\psi_2(z_2) = \psi_{12}(z_2) + \psi_{22}(z_2)$$

$$= -\frac{iT_2 b^2}{z_2} + \frac{iT_1 a^2}{c} - \frac{iT_1 a^2}{(z_2 + c)} + \frac{iT_1 a^2 b^2}{z_2(cz_2 + b^2)^2} \tag{8}$$

They satisfy the boundary condition in Eq. (2) exactly and will give the second approximation to the stresses and displacements valid near hole radius b.

Similarly, the second approximation to the solution which is valid in the vicinity of C_1 can be obtained from similar analysis, starting from the stress functions [Eq. (4)] valid near hole C_2. The transformation $z_2 = z_1 + c$ will give transformed stress functions as

$$\phi_{21}(z_1) = 0 \text{ and } \psi_{21}(z_1) = -iT_2 b^2/(z_1 - c) \tag{9}$$

which would lead to boundary condition f_{21}. Adjusting the required boundary condition on C_1 as $f_1 = +iT_1 t_1 - f_{21}$, the corrected stress functions can be obtained easily. The sum of these two stress functions with Eq. (9) will give the second approximation valid near C_1 and which satisfy the boundary condition in Eq. (1) on C_1 exactly as

$$\phi_1(z_1) = -\frac{iT_2 a^2 b^2}{c(a^2 - cz_1)}$$

$$\psi_1(z_1) = -\frac{iT_1 a^2}{z_1} - \frac{iT_2 b^2}{c} - \frac{iT_2 b^2}{z_1 - c} + \frac{iT_2 a^4 b^2}{z_1(a^2 - cz_1)^2} \tag{10}$$

Third Approximation

The third-order approximation closer to the existing stress field can be easily obtained by following a similar procedure. The stress functions [Eq. (7)] are transformed to the center of hole C_1 and then corrected to satisfy the boundary condition [Eq. (1)] exactly. The sum of the two lead to the third ap-

proximation near the hole of radius a as

$$\phi_1(z_1)=\frac{ia^2(T_1a^2+T_2b^2)}{c(a^2-cz_1)}+\frac{iT_1a^4c^2[3a^2b^2-(c^2-b^2)^2]}{(c^2-b^2)^3[ca^2-(c^2-b^2)z_1]}-\frac{iT_1a^8b^2c^3}{(c^2-b^2)^3[ca^2-(c^2-b^2)z_1]^2}+\frac{iT_1a^2b^2}{c(cz_1-c^2+b^2)} \tag{11}$$

$$\psi_1(z_1)=-\frac{iT_2b^2}{(z_1-c)}+\frac{iT_1a^2b^2}{(z_1-c)(cz_1-c^2+b^2)}-\frac{iT_2b^2}{c}+\frac{ia^4(T_1a^2+T_2b^2)}{z_1(a^2-cz_1)^2}-\frac{iT_1a^2}{z_1}-\frac{2iT_1a^2b^2}{c(c^2-b^2)}+\frac{2iT_1a^4b^2c}{(c^2-b^2)^3}$$

$$+\frac{iT_1a^4b^2}{(c^2-b^2)^2z_1}+\frac{iT_1a^4b^2}{(c^2-b^2)[ca^2-(c^2-b^2)z_1]}-\frac{iT_1a^6c^2[3a^2b^2-(c^2-b^2)^2]}{z_1(c^2-b^2)^2[ca^2-(c^2-b^2)z_1]^2}+\frac{2iT_1a^{10}b^2c^3}{z_1(c^2-b^2)^2[ca^2-(c^2-b^2)z_1]^3}$$

Similarly the third approximation to the stress field valid near the hole of radius b can be obtained as

$$\phi_2(z_2)=-\frac{ib^2(T_1a^2+T_2b^2)}{c(b^2+cz_2)}+\frac{iT_2b^4c^2[(c^2-a^2)^2-3a^2b^2]}{(c^2-a^2)^3[b^2c+(c^2-a^2)z_2]}+\frac{iT_2a^2b^8c^3}{(c^2-a^2)^3[b^2c+(c^2-a^2)z_2]^2}+\frac{iT_2a^2b^2}{c(cz_2+c^2+a^2)} \tag{12}$$

$$\psi_2(z_2)=-\frac{iT_1a^2}{(z_2+c)}-\frac{iT_2a^2b^2}{(z_2+c)(cz_2+c^2-a^2)}-\frac{iT_2a^2b^4}{(c^2-a^2)[cb^2+(c^2-a^2)z_2]}+\frac{iT_2a^2b^4}{(c^2-a^2)^2z_2}+\frac{2iT_2a^2b^2}{c(c^2-a^2)}$$

$$-\frac{2iT_2a^2b^4c}{(c^2-a^2)^3}-\frac{iT_1a^2}{c}-\frac{iT_2b^2}{z_2}-\frac{ib^4(T_1a^2+T_2b^2)}{z_2(b^2+cz_2)^2}+\frac{2iT_2a^2b^{10}c^3}{(c^2-a^2)^2[b^2c+(c^2-a^2)z_2]^3z_2}+\frac{iT_2b^6c^2[(c^2-a^2)^2-3a^2b^2]}{(c^2-a^2)^2z_2[b^2c+(c^2-a^2)z_2]^2}$$

Table 1 Third approximation to the maximum tangential stresses[a] σ_θ around the hole of radius a

	$b/a=1$			$b/a=2$			$b/a=3$			$b/a=4$		
	σ_θ			σ_θ			σ_θ			σ_θ		
d	T_1	T_2	Angle, deg	T_1	T_2	Angle, deg	T_1	T_2	Angle, deg	T_1	T_2	Angle, deg
0.1	−7.235	−2.452	15	−1.883	−3.042	30	−1.206	−3.282	30	−0.916	−3.376	30
0.2	−5.859	−2.027	15	−1.746	−2.794	30	−1.142	−3.007	30	−0.879	−3.218	30
0.4	−3.873	−1.453	15	−1.452	−2.377	30	−0.971	−2.743	30	−0.755	−2.935	30
0.6	−2.66	−1.086	15	−1.192	−2.044	30	−0.807	−2.453	30	−0.629	−2.687	30
0.8	−1.838	−1.002	30	−0.984	−1.775	30	−0.673	−2.206	30	−0.525	−2.469	30
1.0	−1.492	−1.831	30	−0.822	−1.555	30	−0.567	−1.994	30	−0.443	−2.276	30
3.0	−0.342	−0.222	30	−0.233	−0.569	30	−0.175	−0.889	30	−0.141	−1.16	30
5.0	−0.143	−0.990	30	−0.108	−0.29	30	−0.084	−0.512	45	−0.071	−0.728	45
7.0	−0.078	−0.055	30	−0.062	−0.182	45	−0.052	−0.335	45	−0.046	−0.496	45

Table 2 Shearing stresses $\tau_{r\theta}$ at point P[a]

		$b/a=1$		$b/a=2$		$b/a=3$		$b/a=4$	
		T_1	T_2	T_1	T_2	T_1	T_2	T_1	T_2
	F	1.000	+0.825	1.0	+0.906	1.0	+0.937	1.0	+0.453
$d=0.1$	S	1.0	+0.413	1.0	+0.454	1.0	+0.468	1.0	+0.476
	T	7.628	+0.0	2.768	+0.680	6.042	+0.832	18.552	+0.892
	F	1.0	+0.695	1.0	+0.826	1.0	+0.884	1.0	+0.91
$d=0.2$	S	1.0	+0.347	1.0	+0.413	1.0	+0.439	1.0	+0.454
	T	3.33	+0.0	1.231	+0.620	1.237	+0.781	1.191	+0.85
	F	1.0	+0.51	1.0	+0.695	1.0	+0.775	1.0	+0.825
$d=0.4$	S	1.0	+0.255	1.0	+0.345	1.0	+0.389	1.0	+0.431
	T	4.467	+0.0	1.216	+0.521	0.528	−0.692	1.744	−0.61
	F	1.0	+0.39	1.0	+0.592	1.0	+0.693	1.0	+0.756
$d=0.6$	S	1.0	+0.196	1.0	+0.296	1.0	+0.347	1.0	+0.378
	T	3.872	+0.0	1.569	−0.444	0.976	−0.617	0.744	−0.709
	F	1.0	+0.308	1.0	+0.51	1.0	+0.625	1.0	+0.695
$d=0.8$	S	1.0	+0.154	1.0	+0.255	1.0	+0.312	1.0	+0.348
	T	3.304	+0.0	1.635	−0.385	1.146	−0.554	0.94	−0.651
	F	1.0	+0.25	1.0	+0.445	1.0	+0.563	1.0	+0.64
$d=1.0$	S	1.0	+0.125	1.0	+0.225	1.0	+0.281	1.0	+0.32
	T	2.864	+0.0	1.618	−0.333	1.214	−0.5	1.035	−0.60
	F	1.0	+0.062	1.0	+0.160	1.0	+0.25	1.0	+0.327
$d=3.0$	S	1.0	+0.031	1.0	+0.080	1.0	+0.125	—	—
	T	1.431	+0.0	1.2	−0.096	1.166	−0.222	1.112	−0.306
	F	1.0	+0.0028	1.0	+0.0816	1.0	+0.14	1.0	+0.198
$d=5.0$	S	1.0	+0.014	1.0	+0.041	1.0	+0.07	—	—
	T	1.184	+0.0	1.311	−0.061	1.087	−0.125	1.058	−0.185
	F	1.0	+0.00156	1.0	+0.0494	1.0	+0.09	1.0	+0.132
$d=7.0$	S	1.0	+0.008	1.0	+0.025	1.0	+0.045	—	—
	T	1.101	+0.0	1.078	−0.037	1.062	−0.082	−1.082	−0.124

[a] where $d=c-(a+b)/a$ = distance between the two holes, F = first approximation, S = second approximation, and T = third apprroximation.

They satisfy the boundary condition [Eq. (2)] on C_2 exactly.

Numerical Results and Discussion

The numerical results for the distribution of stresses in the plate and the displacements around the hole are obtained with the help of the digital computer EC 1030 at I.I.T. Bombay. The solution converges in three approximations.

It may be noted from Table 1 that maximum tangential stress σ_θ occurs between $\theta_1 = 15$ deg and $\theta_1 = 45$ deg, depending upon the hole radii ratios and their spacing. For example, for $b/a = 2$ and $d = 0.6$ if $T_1 = T_2 = 1.0$, the tangential stress at $r_1 = a$ and $\theta_1 = 30$ deg will be 3.236 and it is compressive in nature. Figure 2 shows the distribution of σ_θ around the hole of radius a.

In Table 2 the values from the first, second, and third approximations are listed for the shearing stress at point P on the boundary of the hole radius a along the line of symmetry. While the radial displacement around the holes is almost zero the tangential displacement u_θ has a distribution similar to σ_θ.

The convergence proof of the Schwarz solution in the solution of the second elastostatic problem for a doubly connected region for the case when the two contours are sufficiently apart has been given by Mikhlim in 1934. A more general proof of the Schwarz algorithm for the second boundary-value problem in three-dimensional elasticity, minimizing the integral for the strain energy, has been given by S. Soboleff in 1936 [Ref. 2, pp. 320-321].

In this Note a new problem has been solved using old methodology, giving interesting results. The first approximations are only one-hole solutions without considering the interaction effect of the other hole. The second approximations are only valid near the respective holes on which they satisfy the exact boundary conditions. The third approximations not only satisfy the boundary conditions on respective holes exactly but also are a very close approximation of the boundary conditions on the other hole. This proves the convergence of the solution of the elastostatic problem whose formulation is consistent with the conditions of this problem.

It may be noted that the solution for the problem of an infinite plate with two clockwise moments M_1 and M_2 applied at the distance of c can be obtained easily from the above solution by taking the limiting case as the radii of the two holes tend to zero or by simple substitution:

$$T_1 = -M_1/2\pi a^2 \text{ and } T_2 = -M_2/2\pi b^2$$

References

[1] Muskhelishvili, N. I., *Some Basic Problems of the Mathematical Theory of Elasticity*, P. Noordhoff Co., Groninger, Holland, 1955.

[2] Sokolnikoff, I. S., *Mathematical Theory of Elasticity*, 2nd ed., McGraw-Hill, New York, 1956.

[3] Kim, T. J. and Ukadgaonker, V.G., "Plane Stress Analysis of Rigid Circular Inclusion," *AIAA Journal*, Vol. 9, Nov. 1971, p. 2294.

[4] Ukadgaonker, V. G., "Stress Analysis of Infinite Plate with Two Rigid Circular Inclusions," *Proceedings of 19th Annual Congress*, Indian Society of Theoretical and Applied Mechanics, held at I.I.T. Kharagpur, India, Dec. 1974, pp. 9-18.

From the AIAA Progress in Astronautics and Aeronautics Series . . .

REMOTE SENSING OF EARTH FROM SPACE: ROLE OF "SMART SENSORS"—v. 67

Edited by Roger A. Breckenridge, NASA Langley Research Center

The technology of remote sensing of Earth from orbiting spacecraft has advanced rapidly from the time two decades ago when the first Earth satellites returned simple radio transmissions and simple photographic information to Earth receivers. The advance has been largely the result of greatly improved detection sensitivity, signal discrimination, and response time of the sensors, as well as the introduction of new and diverse sensors for different physical and chemical functions. But the systems for such remote sensing have until now remained essentially unaltered: raw signals are radioed to ground receivers where the electrical quantities are recorded, converted, zero-adjusted, computed, and tabulated by specially designed electronic apparatus and large main-frame computers. The recent emergence of efficient detector arrays, microprocessors, integrated electronics, and specialized computer circuitry has sparked a revolution in sensor system technology, the so-called smart sensor. By incorporating many or all of the processing functions within the sensor device itself, a smart sensor can, with greater versatility, extract much more useful information from the received physical signals than a simple sensor, and it can handle a much larger volume of data. Smart sensor systems are expected to find application for remote data collection not only in spacecraft but in terrestrial systems as well, in order to circumvent the cumbersome methods associated with limited on-site sensing.

505 pp., 6 × 9, illus., $22.00 Mem., $42.50 List

TO ORDER WRITE: Publications Dept., AIAA, 1290 Avenue of the Americas, New York, N. Y. 10019